

Original citation:

Slater, T.S., Ashbrook, Kate and Kriwet, J. (2020) *Evolutionary relationships among bullhead sharks (Chondrichthyes: Heterodontiformes)*. Papers in Palaeontology. ISSN 2056-2802 (In Press)
<https://doi.org/10.1111/ALL.14168>

Permanent WRaP URL:

<https://eprints.worc.ac.uk/id/eprint/8991>

Copyright and reuse:

The Worcester Research and Publications (WRaP) makes this work available open access under the following conditions. Copyright © and all moral rights to the version of the paper presented here belong to the individual author(s) and/or other copyright owners. To the extent reasonable and practicable the material made available in WRaP has been checked for eligibility before being made available.

Copies of full items can be used for personal research or study, educational, or not-for-profit purposes without prior permission or charge, provided that the authors, title and full bibliographic details are credited, a hyperlink and/or URL is given for the original metadata page and the content is not changed in any way.

Publisher's statement:

This is the accepted manuscript version of the following article: Slater, T.S., Ashbrook, Kate and Kriwet, J. (2020) *Evolutionary relationships among bullhead sharks (Chondrichthyes: Heterodontiformes)*. Papers in Palaeontology. ISSN 2056-2802 (In Press), which has been published in final form at
<https://onlinelibrary.wiley.com/doi/10.1002/spp2.1299> This article may be used for non- commercial purposes in accordance with Wiley Terms and Conditions for Use of Self-Archived Versions.

A note on versions:

The version presented here may differ from the published version or, version of record, if you wish to cite this item you are advised to consult the publisher's version. Please see the 'permanent WRaP URL' above for details on accessing the published version and note that access may require a subscription.

For more information, please contact wrapteam@worc.ac.uk

1
2
3 1 **Evolutionary relationships among bullhead sharks (Chondrichthyes:**
4
5 2 **Heterodontiformes)**

6
7
8 3
9
10 4 by TIFFANY S. SLATER^{1,2*}, KATE ASHBROOK¹, and JÜRGEN KRIWET³

11
12 5
13
14 6 ¹School of Science and the Environment, University of Worcester, Worcester WR2 6AJ, UK;

15
16
17 7 e-mail: k.ashbrook@worc.ac.uk

18
19 8 ²*Current address:* School of Biological, Earth and Environmental Sciences, University

20
21 9 College Cork, Distillery Fields, North Mall, Cork T23 TK30, Ireland; e-mail:

22
23
24 10 tiffany.slater@ucc.ie

25
26 11 ³ University of Vienna, Department of Palaeontology, Althanstraße 14, Wien 1090, Austria;

27
28
29 12 e-mail: juergen.kriwet@univie.ac.at

30
31
32 13
33 14 *Corresponding author

34
35 15
36
37
38 16 **Abstract:** The evolution of modern sharks, skates and rays (Elasmobranchii) is largely
39
40 17 enigmatic due to their possession of a labile cartilaginous skeleton; consequently, taxonomic
41
42 18 assignment often depends on isolated teeth. Bullhead sharks (Heterodontiformes) are a group
43
44 19 of basal neoselachians, thus their remains and relationships are integral to understanding
45
46 20 elasmobranch evolution. Here we fully describe †*Paracestracion danieli* – a bullhead shark
47
48 21 from the Late Jurassic plattenkalks of Eichstätt, Germany (150–154 Ma) – for its inclusion in
49
50 22 cladistic analyses (employing parsimonious principles) using morphological characters from
51
52 23 complete †*Paracestracion* and *Heterodontus* fossil specimens as well as extant forms of the
53
54 24 latter. Results confirm the presence of two separate monophyletic clades within
55
56 25 Heterodontiformes based on predominantly non-dental characters, which show a strong
57
58
59
60

1
2
3 26 divergence in body morphology between †*Paracestracion* and *Heterodontus* (the latter
4
5 27 possessing a first dorsal fin and pectoral fins that are placed more anterior and pelvic fins that
6
7
8 28 are placed more posterior). This study emphasizes the importance of including non-dental
9
10 29 features in heterodontiform systematics (as compared to the use of dental characters alone)
11
12 30 and supports the erection of the family †Paracestracionidae. Further, phylogenetic analysis of
13
14
15 31 molecular data from five extant species suggests that crown heterodontiforms arose from a
16
17 32 diversification event 42.58 Ma off the west coast of the Americas.
18
19 33

20
21 34 **Key words:** elasmobranch evolution, Late Jurassic, Paracestracionidae, *Heterodontus*,
22
23 35 morphology, bullhead sharks
24
25
26 36

27
28 37 CHONDRICHTHYANS have a very long evolutionary history with their earliest fossil
29
30 38 evidence from the Upper Ordovician (Andreev *et al.* 2015). The cartilaginous fishes
31
32 39 include the Holocephali, or modern chimaeroids (Maisey 2012), and the Elasmobranchii
33
34 40 (*sensu* Maisey 2012; = Neoselachii of Compagno 1977), *i.e.* the modern sharks, skates and
35
36 41 rays, which experienced rapid diversification in the Jurassic period and are the
37
38 42 predominant group of living chondrichthyans (Kriwet *et al.* 2009a). Morphological and
39
40 43 molecular studies support two major monophyletic shark clades within Elasmobranchii: the
41
42 44 Galeomorphii and the Squalomorphii (Carvalho & Maisey 1996; Maisey *et al.* 2004;
43
44 45 Winchell *et al.* 2004; Human *et al.* 2006; Mallatt & Winchell 2007; Naylor *et al.* 2012).
45
46 46 Although both groups are well represented in the fossil record, their labile cartilaginous
47
48 47 skeleton leads to a taphonomic bias towards isolated teeth (Kriwet & Klug 2008).
49
50 48 Consequently, much of the early evolutionary history of elasmobranchs is either highly
51
52 49 contested or unknown (Klug 2010).
53
54 50
55
56
57
58
59
60

1
2
3 51 Bullhead sharks (Heterodontiformes) are the most plesiomorphic galeomorphs (Naylor *et*
4
5 52 *al.* 2012), with their remains first appearing in the Early Jurassic (*c.* 175 Ma).

6
7
8 53 Heterodontiforms are therefore among the oldest groups in the fossil record for modern
9
10 54 sharks and have the potential to provide insight into early elasmobranch evolution (Thies
11
12 55 1983; Maisey 2012). Several genera of Heterodontiformes seemingly evolved in the
13
14 56 Jurassic (Kriwet 2008, Hovestadt 2018): †*Proheterodontus*, †*Palaeoheterodontus*,
15
16 57 †*Procestracion* and †*Paracestracion* (all represented by isolated teeth and the last also by
17
18 58 complete specimens) disappear from the fossil record before the Cretaceous, while
19
20
21 59 *Heterodontus* underwent further radiation and still occupies our waters today (Kriwet
22
23 60 2008). †*Protoheterodontus* briefly appears in the Campanian (Guinot *et al.* 2013,
24
25 61 Hovestadt 2018) but did not make a significant contribution to Late Cretaceous
26
27 62 biodiversity.

28
29
30
31 63
32
33 64 Bullhead sharks possess a durotrophic littoral ecomorphotype and are characterized by a
34
35 65 distinct heterodont dentition with cuspidate anterior teeth to grab invertebrate prey and
36
37 66 robust and flattened posterior teeth to crush armoured prey items or small bony fish (Strong
38
39 67 1989; Maia *et al.* 2012). The Eichstätt and Solnhofen areas in southern Germany (and
40
41 68 Dover in the U.K.) formed part of an archipelago in the Jurassic that was surrounded by
42
43 69 shallow waters of the Tethys Sea (Kriwet & Klug 2008), which likely promoted allopatric
44
45 70 speciation in heterodontiforms (Cuny & Benton 1999). Understanding the evolutionary
46
47 71 history and past taxonomic diversity of elasmobranchs, however, is encumbered by
48
49 72 preservation and collecting biases (Guinot & Cavin 2015).

50
51
52
53
54 73
55
56 74 Completely articulated specimens of elasmobranchs are of utmost importance because they
57
58 75 provide abundant anatomical characters for exact taxonomic identification and can inform
59
60

1
2
3 76 on morphological, ontogenetic and ecological adaptive changes in their evolution. Here we
4
5 77 provide a formal description of †*Paracestracion danieli* – a subadult specimen from the
6
7
8 78 Tithonian of Eichstätt, Germany (150–154 Ma) that was previously identified as a new
9
10 79 species (Slater 2016).

11
12 80
13
14 81 Relationships within Heterodontiformes have received surprisingly little attention despite
15
16 82 their important phylogenetic position (Maisey 1982, 2012), with recent work including
17
18 83 only dental characters (Hovestadt 2018). Anatomical characters from †*Paracestracion* and
19
20 84 *Heterodontus* fossils, as well as extant species from the latter, were used in cladistic
21
22
23 85 analyses to examine the evolutionary relationships within heterodontiforms. Taxa based on
24
25 86 teeth alone were not included here and, despite recent advances (Hovestadt 2018), their
26
27 87 validity remains untested. A taxonomic diversity analysis based solely on extinct and extant
28
29 88 heterodontid dentition was, however, performed using data from Hovestadt (2018) and Reif
30
31 89 (1976) for comparison. Additionally, the phylogenetic relationships of extant *Heterodontus*
32
33 90 were investigated using molecular data from five species. Elucidation of the
34
35
36
37 91 interrelationships of heterodontiforms will help inform key questions regarding the
38
39 92 biodiversity and evolutionary history of heterodontiforms.

93 94 MATERIAL AND METHODS

95 *Taxonomic analysis of †Paracestracion danieli*

96 Ultraviolet light was used to expose delicate fossil structures in †*Paracestracion danieli*.

97 High-resolution casts were made of significant anatomical features, such as teeth and placoid
98 scales, which were photographed using a KEYENCE 3D Digital VHX-600 microscope.

99 100 *Multivariate statistical analysis of heterodontids*

1
2
3 101 Seven distance measurements were taken from †*Paracestracion danieli*, †*P. falcifer* (AS-
4
5 102 VI-505), extant juveniles of *H. japonicus*, *H. zebra*, *H. portusjacksoni* and two adult *H.*
6
7 103 *japonicus* to identify differences in body shape between genera (Slater *et al.* 2019, table
8
9 104 S1, S2). Measurements taken were total body length, length between the anterior and
10
11 105 posterior dorsal fin, length between posterior dorsal fin and caudal fin, distance between
12
13 106 the pectoral fin and pelvic fin, length between the pelvic fin and anal fin, and widths of the
14
15 107 pectoral and pelvic girdle. Distance measurements were corrected for allometry in the
16
17 108 software package PAST v.3.20 (Hammer *et al.* 2001) and a Principal Components
18
19 109 Analysis (PCA) was performed.
20
21
22
23
24 110

25 111 *Cladistic analysis of heterodontiforms*

26 112 Three extant species of *Heterodontus* and fossil specimens of †*Paracestracion*,
27
28 113 *Heterodontus* and †*Palaeospinax* – a stem-group representative of Elasmobranchii used to
29
30 114 polarize characters (Klug 2010) – were examined to create a robust character matrix
31
32 115 (Harvey & Pagel 1991; see Slater *et al.* 2019 for information on specimens used in this
33
34 116 study). Morphological trait analysis was carried out using the protocol from Klug (2010).
35
36 117 Irrelevant and particularly labile characters were removed and characters specific to
37
38 118 Heterodontiformes were added: two cranial (#96, 103), 15 postcranial (#94, 97–102, 104–
39
40 119 112), two fin spine (#93, 113), 13 dental (#76–80, 83–84, 86–91) and one denticle
41
42 120 character (#92).
43
44
45
46
47
48
49 121

50
51 122 A total of 113 characters were used to create a character matrix in the software program
52
53 123 Mesquite v.3.51 (Maddison & Maddison 2018). Morphological characters from
54
55 124 †*Palidiplospinax* were all coded as [0] (Klug 2010). Soft tissue characters were removed
56
57 125 from the matrix prior to analysis and characters that were not applicable to a specimen
58
59
60

1
2
3 126 (such as the presence of molariform teeth in juvenile heterodontids or in the absence of
4
5 127 preservation) were coded as [?]. Parsimonious approaches were used in the software
6
7
8 128 program PAUP* v4.0 and 1000 replicates were performed using the heuristic search mode
9
10 129 by stepwise addition to obtain bootstrap values (Felsenstein 1985; Swafford 2002). All
11
12 130 characters were treated with equal weight. Both ACCTRAN and DELTRAN algorithms
13
14
15 131 were used as they assign character changes as closely as possible to the nodes and tips,
16
17 132 respectively (Agnarsson & Miller 2008). Sixty phylogenetically uninformative and/or
18
19 133 constant characters were removed (#1–17, 19–26, 28, 30–39, 42–48, 50–51, 53–57, 62,
20
21 134 64–65, 67, 70, 73, 75–76, 104, 112).

135

136 *Taxonomic diversity analysis*

137 The standing diversity of heterodontiforms was determined for species presented in
138 Hovestadt (2018). Genera of ambiguous systematic position within Heterodontiformes
139 were omitted and 95% confidence intervals (CI) were calculated to obtain a measure for
140 the significance of results. We also consider the stratigraphic distribution of the two dental
141 morphotypes proposed for extant and extinct heterodontiforms by Reif (1976) and
142 Hovestadt (2018).

143

144 *Molecular phylogeny of extant heterodontids*

145 Homologous NADH2 mitochondrial gene sequences for *Chimaera phantasma* (accession
146 number JQ518719.1), *Torpedo fuscomaculata* (JQ518934.1), *Raja montagui* (JQ518886.1),
147 *Heterodontus galeatus* (JQ518722.1), *H. portusjacksoni* (JQ519033.1), *H. zebra*
148 (KF927894.1), *H. mexicanus* (JQ519166.1) and *H. francisci* (JQ519165.1) were aligned using
149 ClustalW in MEGA v7.0 (Kumar *et al.* 2016). *C. phantasma* was used as the outgroup and a
150 maximum likelihood phylogeny was produced using a GTR+ Γ model and an analytical

1
2
3 151 variance estimation with nucleotide substitutions and a strong branch swap filter. Gaps and
4
5 152 missing data were treated as complete deletions and 1000 bootstrap replications were
6
7
8 153 executed. A time tree was constructed using a local clock and a minimum and maximum
9
10 154 divergence date between Rajiformes and Torpediniformes (187.8–209 Ma) for calibration
11
12 155 (Inoue *et al.* 2010; Aschliman *et al.* 2012).

156

157 GEOGRAPHICAL AND GEOLOGICAL SETTING

158 †*Paracestracion danieli* (PBP-SOL-0005) was excavated from the Solnhofen limestone
19
20
21
22
23 159 (ca. 153 Ma, early Tithonian, Late Jurassic) near Eichstätt (South Germany; Fig. 1). The
24
25 160 fossil-yielding layers consist of finely laminated and strongly silicified calcarenites and
26
27 161 calcisiltites (for information about the geology and geography of this area see Kriwet &
28
29 162 Klug 2004).

163

33
34 164 *Institutional abbreviations.* BSPG, Bayerische Staatssammlung für Paläontologie und
35
36 165 Geologie Munich, Germany; JME, Jura Museum Eichstätt, Germany; SMNS, State
37
38 166 Museum of Natural History Stuttgart, Germany; PBP-SOL, Wyoming Dinosaur Center,
39
40 167 USA.

168

169 SYSTEMATIC PALAEOLOGY

46
47
48 170 Superclass CHONDRICHTHYES Huxley, 1880

49
50 171 Class ELASMOBRANCHII Bonaparte, 1838

51
52
53 172 Cohort EUSELACHII Hay, 1902

54
55 173 Subcohort NEOSELACHII Compagno, 1977

56
57 174 Superorder GALEOMORPHII Compagno, 1973

58
59 175 Order HETERODONTIFORMES Berg, 1940
60

1
2
3 176 Family PARACESTRACIONIDAE

4
5 177 *LSID*. urn:lsid:zoobank.org:act:XXXXXXXXXX

6
7
8 178

9
10 179 Genus †PARACESTRACION Koken, in Zittel, 1911

11
12 180

13
14
15 181 *Type species*. †*Cestracion falcifer* Wagner, 1857 (BSPG AS-VI-505); lower Tithonian of
16
17 182 Solnhofen, South Germany.

18
19 183

20
21 184 †*Paracestracion danieli*

22
23
24 185 Figure 2

25
26 186

27
28 187 *Derivation of name*. Named in honour of J. Frank Daniel for his work on the endoskeleton of
29
30
31 188 **extant** heterodontiform sharks.

32
33 189

34
35 190 *Holotype*. PBP-SOL-0005, complete specimen preserved in part and counterpart.

36
37
38 191

39
40 192 *Diagnosis*. †*P. danieli* is characterized by the following combination of plesiomorphic and
41
42 193 autapomorphic (indicated by an asterisk) morphological traits: **labial ornamentation** on
43
44 194 **anterior teeth**; absence of distal curvature in parasymphyseal teeth; pectoral girdle positioned
45
46 195 at the 12th vertebra*; and first dorsal fin spine placed at the 32nd and 33rd vertebrae*.

47
48
49 196

50
51 197 *Description*. **The part and counterpart of †*P. danieli* display organic preservation of the body**
52
53 198 **shape and a complete and fully articulated cartilaginous skeleton** (Fig. 2A–B). **The paired fins**
54
55 199 **are represented by a single fin each: the pectoral fin is ovular in shape (i.e. possesses no**
56
57 200 **distinct margins) and is most broad near its trailing edge, while the pelvic fin – ventral to the**

58
59
60

1
2
3 201 anterior dorsal fin and abutting the pectoral fin – is pointed at both its apex and free rear tip
4
5 202 and has an anterior and posterior margin of similar length. The anterior dorsal fin (height, 23
6
7
8 203 mm; length, 40.4 mm) is larger than the posterior (height, 25.9 mm; length, 30.2 mm) but
9
10 204 both possess a rounded apex and a gently curved posterior margin. The anal fin is ventral to
11
12 205 the posterior dorsal fin, is its own length to the caudal fin and is pointed at its apex. A pointed
13
14 206 ventral tip joins the pre- and postventral margin of the caudal fin, with the postventral margin
15
16 207 extending dorsocaudally to a ventral posterior tip. The dorsal lobe predominates the caudal
17
18 208 fin, whereby the upper postventral margin continues anterodorsally to a broad subterminal
19
20
21 209 notch. The posterior margin and the dorsal posterior ‘tip’ are rounded and possess no distinct
22
23
24 210 boundaries.

25
26 211
27
28 212 A dense layer of denticles obstructs the view of the neurocranium. The hyomandibula, hyoid
29
30
31 213 and branchial apparatus are embedded in sediment. Segments of the Meckel’s cartilage join at
32
33 214 the symphysis to form a bulbous rostrum and then extend in a posterolateral fashion (Fig. 2C).
34
35 215 One mandible segment is fully exposed in lateral view and maintains a similar height along its
36
37
38 216 entire length; the posterior end does not possess a strong process but is negatively cambered
39
40 217 (i.e. the ventral margin extends more laterally than the dorsal margin) before it curves
41
42 218 dorsally to form the quadrato-mandibular joint. Features of the palatoquadrate are obscured
43
44 219 by sediment. Two dorsal fin spines are positioned directly anterior to each dorsal fin (Fig.
45
46 220 3A–B). The posterior fin spine is larger and more recurved than the anterior and the caps of
47
48 221 each bear no tuberculation. Skeletal features such as the propterygium, mesopterygium and
49
50
51 222 metapterygium are visible, however much of their features are embedded in the sediment.
52
53
54 223 Supraneural elements are present and are along the posterior end of the caudal fin.
55
56 224

57
58 225 Exposed teeth on the Meckel’s cartilage are preserved *in situ* and are symmetrical and possess
59
60

1
2
3 226 a gentle slope. Three small, lateral cusps flank each side of a large, central cusp – all of which
4
5 227 possess distinct vertical striations on their labial face (Fig. 2D–F). The pair of cusps most
6
7
8 228 proximal to the central cusp are well developed when compared to the other cusplets. The
9
10 229 cusps are not lingually bent and the lateral and posterior teeth are not distally inclined.
11
12 230 Anterior teeth are taller than they are wide and exhibit a slightly convex basal labial edge that
13
14 231 juts out over the crown/root junction (Fig. 2E–F). Lateral teeth are wider than they are tall,
15
16 232 and the basal labial edge is less prominent than in anterior teeth (Fig. 2D). No molariform
17
18 233 teeth are present, which supports that the specimen is subadult. The root is gently curved in
19
20 234 basal view and the vascularisation is of the holaulacorhize type. Single, circular nutritive
21
22 235 foramina are located in the centre of a nutritive groove, which divides the root into two lobes
23
24 236 (Fig. 2G). No nutritive foramina are visible on the lateral faces of the root lobes.
25
26
27
28
29
30

31 238 The most rostral part of the cranium is densely covered in denticles that are preserved in
32
33 239 apical view and have a slightly convex crown surface and a wide posterior margin that gently
34
35 240 tapers to a rounded anterior tip (Fig. 2H). Denticle crowns on the rest of the cranium possess
36
37 241 (in apical view) a delicate mid-ridge and an arrow-like morphology that is nearly as wide as it
38
39 242 is long (Fig. 2I); the ventral side of the body is flanked with denticles of similar morphology
40
41 243 but are longer than they are wide (and thus are more pointed at their apex) and have a more
42
43 244 prominent mid-ridge in apical aspect (Fig. 2J). Denticles along the anterior margins of the
44
45 245 paired fins are again arrow-like in shape but have a weak mid-ridge and a much shorter ‘stem’
46
47 246 than cranial and ventral denticles (Fig. 2K). Many dorsal denticles possess the same
48
49 247 morphology as those on the ventral side of the body; some, however, are thorn-like in apical
50
51 248 view (Fig. 3C). Anterior to the fin spines are dorsal thorns, which – unlike denticles – sit
52
53 249 perpendicular to the body, are slightly concave in lateral view and have a broad base that
54
55 250 tapers to a sharp, recurved apex (Fig. 3D).
56
57
58
59
60

251

252 *Occurrence.* Late Jurassic (Tithonian, ca. 153 Ma).

253

254 RESULTS

255 *Comparison and multivariate statistical analysis of meristic characters*

256 †*Paracestracion danieli* is characterized by seven cusps in anterior teeth at a body length of
257 225 mm while the holotype of †*P. falcifer* (AS-VI-505) exhibits a single cusp in anterior teeth
258 at a body length of 400mm (Fig. 4). The position of various features along the body column
259 (e.g. at the n^{th} vertebrae) are markedly different between †*P. danieli* and †*P. falcifer*: the
260 dorsal fin spines in the former (anterior: 32nd–33rd; posterior: 62nd–63rd) – as well as the
261 pectoral and pelvic girdle (12th and 32nd, respectively) – are placed more posterior along the
262 body when compared to †*P. falcifer* (anterior fin spine: 23rd–24th; posterior fin spine: 43rd–
263 44th; pectoral and pelvic girdle: 10th and 24th, respectively; Slater 2016, table 1). This is
264 confirmed by multivariate statistical analysis, which reveals that the distance between the
265 pectoral and pelvic fins accounts for the majority of the variation (PC1=78.9%) in body shape
266 between †*P. danieli*, †*P. falcifer* as well as extant species of *Heterodontus*: the distance
267 between the posterior dorsal and caudal fin (PC2) explain 15.9% of the variation (Fig. 5).

268

269 *Cladistic analysis of heterodontiforms*

270 The cladistic analysis produced one most parsimonious tree with a tree length of 61, a
271 consistency index of 0.9016 (indicating a low amount of homoplasy in the dataset) and a
272 retention index of 0.9062 (indicating that the proportion of terminal taxa retaining the
273 character identified as a synapomorphy is high). Unless specified, characters were assigned
274 to nodes and terminal taxa by both ACCTRAN and DELTRAN optimizations. Results from

1
2
3
4
5
6
7
8
9
10
11
12
13
14
15
16
17
18
19
20
21
22
23
24
25
26
27
28
29
30
31
32
33
34
35
36
37
38
39
40
41
42
43
44
45
46
47
48
49
50
51
52
53
54
55
56
57
58
59
60

1
2
3 275 our analysis support two monophyletic groups, a clade that includes †*Paracestracion*
4
5 276 species and one that contains extinct and extant forms of *Heterodontus* (Fig. 6).
6
7

8 277
9
10 278 Characters supporting the monophyly of node B are the presence of a root shelf that
11
12 279 surrounds the entire circumference of the tooth (likely anchoring them in the mucosal
13
14 280 tissue), pelvic fins that are ventral to the first dorsal fin and, as assigned by ACCTRAN
15
16 281 optimization, abutting the pectorals (Fig. 6). The vertebrae above which the first dorsal fin
17
18 282 spine is inserted is considered an autapomorphic character for †*P. viohli*, †*P. falcifer* and
19
20
21 283 †*P. danieli* (22–23rd, 24–25th and 32–33rd vertebrae, respectively).
22
23
24 284

25
26 285 Node C is characterized by pelvic fins that abut the pectorals and seven cusps on the
27
28 286 symphyseal teeth as a juvenile, which are both supported by DELTRAN optimization.
29
30
31 287 Specimen SMNS 11150 is identified as a separate species from †*P. falcifer* due to the
32
33 288 presence of five cusps on its anterior teeth as a juvenile (ACCTRAN optimization; Fig.
34
35 289 S1). †*Paracestracion viohli* (JME Sha 728) is characterized by ornamentation on the
36
37 290 lingual tooth crown face and a lack thereof on the labial face in anterior teeth.
38
39
40 291

41
42 292 Node D features dorsal thorns (DELTRAN optimization) and an absence of distal curvature
43
44 293 in the parasymphyseal teeth of juveniles. †*Paracestracion danieli* features an additional two
45
46 294 characters: a pectoral girdle at the 12th vertebra and the aforementioned position of the first
47
48 295 dorsal fin spine.
49

50
51 296
52
53
54 297 Node E identifies a monophyletic clade that is supported by a low number of tooth families
55
56 298 (≤ 21) (ACCTRAN optimization), an absence of labial tooth crown ornamentation in
57
58 299 anterior teeth, an anal fin that is more than its own length in distance to the caudal fin and a
59
60

1
2
3 300 pectoral girdle positioned at the eighth vertebrae. †*Heterodontus zitteli* features accessory
4
5 301 cusplets that are nearly the same height as the central cusp and – as in †*P. danieli* – dorsal
6
7
8 302 thorns (DELTRAN optimization) and seven cusps on the anterior teeth (DELTRAN
9
10 303 optimization).
11
12 304
13
14 305 Node F features an absence of a horizontal root on the basal face of anterior teeth, labial
15
16 306 faces of the crown that jut out over the crown/root junction, anterior teeth with a convex
17
18 307 labial face, absence of a cylindrical central cusp, presence of a medio-lingual protuberance,
19
20
21 308 and an absence of fin spine tuberculation. Additional characters are identifiable when
22
23
24 309 ACCTTRAN optimization is used: an anal fin that is posterior to the second dorsal fin,
25
26 310 absence of dorsal thorns, pectoral fins that are entirely situated anterior to the first dorsal
27
28 311 fin, and a high number of vertebral centra. DELTRAN optimization also identifies a low
29
30
31 312 number of tooth rows to this node. †*Heterodontus canaliculatus* is recognized by
32
33 313 ACCTTRAN as having three cusps in adult anterior teeth.
34
35 314
36
37 315 Node G is exclusive to extant *Heterodontus* and shows a relationship between species
38
39 316 occupying shallow waters off of the coasts of Australia and the east coast of Asia.
40
41 317 Characters for node G include: two root lobes are inclined and join in the midline of the
42
43 318 lingual side of the tooth, broad molariform teeth with no median crest on the cutting edge
44
45
46 319 in adults, an anal fin that is posterior to the second dorsal fin, pectoral fins that are not
47
48 320 situated anterior to the first dorsal fin, a low number of vertebrae and a single cusp in adult
49
50
51 321 anterior teeth (the last of which is supported by DELTRAN optimization). *Heterodontus*
52
53
54 322 *portusjacksoni* has enameloid ridges on molariformes, a less pronounced supraorbital crest,
55
56 323 and five cusps in juvenile anterior teeth (the last is supported by ACCTTRAN optimization).
57
58 324 *H. japonicus*, conversely, has seven cusps in juvenile anterior teeth.
59
60

325

326 *Taxonomic diversity of heterodontiforms*

327 Analysis of data from Hovestadt (2018) shows that the standing taxonomic diversity of
 328 fossil heterodontiforms increased from the Early to the Late Jurassic, followed by a 1.7%
 329 decrease in species across the Jurassic/Cretaceous boundary (Table 1). The Late
 330 Cretaceous represents 26.3% of the total extinct and extant taxonomic diversity for
 331 heterodontiforms, with the Cenomanian accounting for most species. Further, an 8.8%
 332 decrease in species standing diversity occurs across the K/Pg boundary but is not
 333 significant. The Palaeogene represents 17.5% of the total diversity of fossil and extant
 334 heterodontiforms, while the Neogene represents 12.3%. Three and six extant species
 335 display dental structures of morphotype 1 and 2, respectively.

336

337 *Molecular phylogeny of extant Heterodontus*

338 Results indicate that *H. francisci* – originating ca. 42.58 Ma – is basal to all other extant
 339 heterodontids included in our analysis and that *H. mexicanus* and *H. zebra* diverged from *H.*
 340 *francisci* ca. 27.67 Ma and 9.22 Ma, respectively (Fig. 7). *H. portusjacksoni* and *H. galeatus*
 341 are shown to have diverged from each other 7.14 Ma. The low bootstrap support value,
 342 however, indicates that their relationships remain unresolved.

343

344 **DISCUSSION**345 *Comparison of Heterodontidae and †Paracestracionidae*

346 Cladistic analysis and comparison of dental and non-dental features between *Heterodontus*
 347 and †*Paracestracion* supports the necessity for a family – †*Paracestracionidae* – to include
 348 all extinct forms of the latter.

349

350

1
2
3 350 *Post-cranial features*. Our findings emphasize the differences in body morphology between
4
5 351 Heterodontidae and †Paracestracionidae and characterizes the latter as having pelvic fins that
6
7
8 352 are placed more anterior as well as a first dorsal fin that is placed more posterior – two key
9
10 353 features that are possessed by slow swimming epibenthic and benthic sharks (Figs 5, 6; Maia
11
12 354 *et al.* 2012). In contrast, traits that are generally associated with a more active lifestyle, such
13
14
15 355 as a (1) first dorsal fin and associated fin spine that are placed more anterior (2) pelvic girdle
16
17 356 and fins that are placed more posterior and (3) pectoral girdle that is placed more anterior,
18
19 357 are most clearly manifested in the Heterodontidae. The Late Jurassic culminated in a
20
21 358 radiation in teleosts (Arratia 2004) as well as marine transgressions and minor mass
22
23
24 359 extinctions that primarily affected coastal reef habitats (Hallam 1981, 1990, 2001; Moore &
25
26 360 Ross 1994), which would have led to an increase in competition; it is plausible that the body
27
28 361 morphology of *Heterodontus* contributed to their persistence into the Cretaceous, unlike
29
30
31 362 *Paracestracion*.
32
33 363
34
35 364 †*Paracestracion* has previously been defined by the position of the pelvic fins, whereby they
36
37
38 365 abut the pectorals and sit below the first dorsal fin (Kriwet *et al.* 2009b). Interestingly, the
39
40 366 first dorsal fin spine's position along the vertebral column unambiguously distinguishes †*P.*
41
42 367 *falcifer* and †*P. danieli*. Although this is also an autapomorphic character for †*P. vohli*
43
44 368 sexual dimorphism cannot be ruled out (compare Daniel 1915) due to its missing posterior
45
46
47 369 end and is therefore only characterized by its dental ornamentation in this study. Further, †*P.*
48
49 370 *falcifer* (the holotype) and †*P. danieli* possess thorns. This trait, however, is also present in
50
51 371 †*H. zitteli* and similar structures present in juvenile angel sharks are lost as they age
52
53
54 372 (Compagno 2001). Investigation of the presence/absence of dorsal thorns in undoubtedly
55
56 373 adult heterodontiforms is thus necessary to determine if it is an ontogenetic or a homoplastic
57
58 374 feature.
59
60

1
2
3 375
4
5 376 *Dentition*. This study identifies an additional key characteristic of †Paracestracionidae
6
7
8 377 those of previous studies (Kriwet *et al.* 2009b): teeth exhibit a root shelf whereas in
9
10 378 Heterodontidae the root lobes meet in the midline of the tooth and form a lingual
11
12 379 protuberance. Additionally, the rate at which the number of cusps is reduced throughout
13
14 380 ontogeny in extant Heterodontidae is very gradual when compared to †Paracestracionidae
15
16 381 (Reif 1976; Fig. 3). The Meckel's cartilage and palatoquadrate in extant juveniles contains
17
18 382 13–17 and 17–21 tooth families, respectively (Reif 1976), while †*P. danieli* possesses 21 and
19
20 383 23 families, respectively, and the holotype for †*P. falcifer* possesses 29 on the palatoquadrate:
21
22
23 384 this may indicate a major difference in feeding ecology between Heterodontidae and
24
25 385 †Paracestracionidae (Slater 2016). Further studies on the ontogeny of heterodonty in
26
27 386 Heterodontiformes, however, are required to confidently determine differences in dentition
28
29
30 387 between the two families and examine the impact on their evolutionary fates.
31
32
33 388

34 35 389 *Taxonomy of Heterodontiformes*

36
37
38 390 Extant species of *Heterodontus* are divided into two groups based on tooth morphology (Reif
39
40 391 1976): following this concept, Hovestadt (2018) revises extant and extinct heterodontiform
41
42 392 systematics and assigns fossil species to either morphotype 1 or 2 (corresponding to the
43
44 393 *Portusjacksoni* and *Francisci* group, respectively, of Reif 1976 for extant species) or, if a
45
46 394 combination of characters is present, to a new genus. New genera based exclusively on
47
48 395 isolated fossil teeth were thus introduced: †*Protoheterodontus* is represented by a single
49
50 396 occurrence from the Campanian (Late Cretaceous) of France (Guinot *et al.* 2013),
51
52
53 397 †*Palaeoheterodontus* by a species in the late Late to early Middle Jurassic and
54
55 398 †*Procestracion* by a single anterior tooth from the Kimmeridgian of southern Germany
56
57 399 (Hovestadt 2018). Further, Hovestadt (2018) assumes †*Cestracion zitteli* to be undiagnosable
58
59
60

1
2
3 400 (*nomina nuda*) due to an absence of preserved dentition and considers †*P. viohli* Kriwet, 2008
4
5 401 as a non-heterodontiform due to the lack of associated dental characters (p. 90). However, in
6
7
8 402 this study, we show that – in addition to dental features – non-dental characters clearly
9
10 403 identify †*Paracestracion zitteli* to represent the most basal member of heterodontids and
11
12 404 support the inclusion of †*P. viohli* in †Paracestracionidae. Ultimately, systematic assignment
13
14 405 of heterodontiforms based on dental characters alone is likely to provide ambiguous results
15
16 406 due to an absence of data on the ontogeny of heterodonty as well as the prevalence of
17
18 407 convergent evolution in elasmobranch dentition. Our study utilizes non-dental features to
19
20
21 408 distinguish several species within the Heterodontiformes and thus highlights the importance
22
23 409 of these characters in taxonomic analyses of heterodontiform fossils.
24
25
26 410

27
28 411 A new Super Order (Paracestracioniformes) and family (Paracestracionidae) was proposed
29
30 412 (Jacques and Van Waes 2012) to include all members of the †*Paracestracion* genus however
31
32 413 neither was registered. Our study confirms the necessity for the family †Paracestracionidae
33
34 414 however we refrain from introducing a new order to include the †Paracestracionidae family
35
36
37 415 due to the restriction of taxa in our analyses, which does not reject the interpretation that both
38
39 416 families represent sister groups within Heterodontiformes.
40
41
42 417

43 44 418 *Diversity patterns of heterodontiforms*

45
46 419 A 1.7% decrease in species across the Jurassic/Cretaceous boundary is likely due to the
47
48 420 limited number of species recorded in the Early Cretaceous, which may be a result of
49
50 421 collecting bias: consequently, a significant decrease in heterodontiform diversity across the
51
52
53 422 Jurassic/Cretaceous boundary cannot be unambiguously established. The Late Cretaceous
54
55 423 heralds the highest species diversity in the evolutionary history of heterodontiforms however
56
57 424 it is unbalanced among the epochs and is generally rather low.
58
59
60

425

426 *Relationships within extant heterodontiforms*427 *Origins of crown heterodontiforms.* Divergence dates in this study are based on the minimum

428 and maximum divergence dates between Rajiformes and Torpediniformes, which spans

429 187.8–209 Ma. Our estimate that crown heterodontiforms originated with *H. francisci* off the

430 west coast of the Americas ca. 42.58 Ma largely supports a previous estimate of 47 Ma

431 (Sorenson *et al.* 2014). *Heterodontus quoyi* (not included in this study) also occupies waters

432 off the west coast of South America and was previously posited as the most plesiomorphic

433 heterodontid due to the proximity of the anal fin to the caudal fin – as in †*H. zitteli* (Maisey434 1982). It is therefore critical to obtain molecular information for *H. quoyi* to elucidate the

435 origin of crown heterodontiforms.

436

437 Ultimately, our molecular phylogeny suggests that pre-Eocene – and especially Cretaceous

438 heterodontiforms – represent stem group members. This contrasts with Hovestadt (2018), in

439 which (apart from the absence of morphotype 2 from the Oligocene) both dental morphotypes

440 are present in the Palaeogene, Neogene and the Late Cretaceous (Table 1). If dentitions bear

441 not only a taxonomic but also a phylogenetic signal – which remains to be tested – this would

442 indicate that species resembling modern heterodontiforms evolved in the late Early

443 Cretaceous. Our results are, nevertheless, consistent with the data from Hovestadt (2018) that

444 indicate that morphotype 2 (Francisci group of Reif 1976) is the most plesiomorphic of

445 heterodontiform dentitions. We, however, consider the reconstruction of heterodontid

446 evolution based on dental features alone insufficient: molecular information combined with

447 morphological evidence from complete fossil specimens provides a larger, more robust

448 dataset than one based on dental morphology.

449

1
2
3 450 *Eastern Pacific species*. During the mid-Eocene shallow waters of the Tethys Sea extended to
4
5 451 what are presently the west coasts of the Americas, the east coast of North America and the
6
7
8 452 Gulf of Mexico and the disparity in the oceanic temperature from the equator to the poles was
9
10 453 reduced (Barron 1987; Sluijs *et al.* 2006; Hines *et al.* 2017): these conditions may have
11
12 454 contributed to the migration and subsequent speciation of heterodontids during the mid-
13
14
15 455 Eocene due to their strong preference for waters over 21 °C (Compagno 2001).

16 456
17
18 457 *Western Pacific species*. Results also reveal a monophyletic relation for species along the east
19
20
21 458 Asiatic and Australian coasts (*H. zebra*, *H. portusjacksoni* and *H. galeatus*): future
22
23
24 459 palaeontological discoveries might clarify the migration routes resulting in the divergence of
25
26 460 these species (as well as those not included in this study along the east coast of Saudi Arabia
27
28 461 and Africa) from those in the Eastern Pacific ca. 9.22 Ma (Ebert *et al.* 2017; Pollom *et al.*
29
30
31 462 2019). The topology of Western Pacific species in our phylogeny is likely different from that
32
33 463 of Naylor *et al.* (2012) due to their use of Bayesian principles: further, the positions of *H.*
34
35 464 *portusjacksoni* and *H. galeatus* are considered unresolved here.

36
37 465

38 466 CONCLUSIONS

39
40
41 467 Anatomical characters from complete bullhead shark fossils support the monophyly of
42
43
44 468 Heterodontiformes, which can be separated into two families: one including solely extinct
45
46
47 469 forms of †*Paracestracion* – assigned to †Paracestracionidae – and both extinct and extant
48
49 470 forms of *Heterodontus* within the Heterodontidae. Although we recognize the importance of
50
51 471 tooth morphologies in taxonomic analyses the phylogenetic signal of heterodontiform dental
52
53
54 472 characters requires further investigation. This study emphasizes the importance of using non-
55
56 473 dental features to provide a greater number of informative characters when investigating the
57
58 474 systematics of chondrichthyan fossils.

59
60

1
2
3 475
4
5 476 Molecular phylogenetic analysis reveals that crown heterodontiforms likely originated off the
6
7
8 477 west coast of the Americas due to a diversification event during the mid-Eocene. Further
9
10 478 research, however, is required to elucidate the evolutionary history of Heterodontiformes and
11
12 479 to clarify migration routes that led to the current distribution of *Heterodontus*.

13
14 480
15
16
17 481 *Acknowledgements.* We are grateful for the Palaeontological Association Undergraduate
18
19 482 Research Bursary PA-UB201606 that financially supported T.S. on this project. We thank B.
20
21 483 Pohl (Wyoming Dinosaur Center), P. Bartsch and J. Klapp (Museum für Naturkunde Berlin)
22
23
24 484 and E. Bernard (London Natural History Museum) for access and assistance with their
25
26 485 collections and G. Cuny for useful comments on the manuscript.

27
28 486

31 487 **DATA ARCHIVING STATEMENT**

32
33 488 Data for this study are available in the Dryad Digital Repository:

34
35 489 <https://datadryad.org/review?doi=doi:10.5061/dryad.6p4f83q>

36
37
38 490 This published work and the nomenclatural act it contains, have been registered in ZooBank:

39
40 491 <http://zoobank.org/References/XXXXXXXXXX>

41
42 492

43 44 493 **REFERENCES**

45
46
47 494 AGNARSSON, I. and MILLER, J. A. 2008. Is ACCTRAN better than DELTRAN?

48
49 495 *Cladistics*, **24**, 1–7.

50
51 496

52
53
54 497 ANDREEV, P. S., COATES, M. I., SHELTON, R. M., COOPER, P. R., SMITH, M. P.,

55
56 498 SANSOM and SANSOM, I. J. 2015. Upper Ordovician chondrichthyan-like scales from

57
58 499 North America. *Palaeontology*, **58**, 691–704.

59
60

1
2
3 5004
5 501 ARRATIA, G. 2004. Mesozoic halecostomes and the early radiation of teleosts. 279–315. *In*6
7 502 ARRATIA, G. and TINTORI, A. (eds.). *Mesozoic Fishes 3 – Systematics, Paleoenvironments*8
9 503 *and Biodiversity*. Dr Friedrich Pfeil Verlag, München, 649 pp.10
11
12 50413
14 505 ASCHLIMAN, N. C., NISHIDA, M., MIYA, M., INOUE, J. G., ROSANA, K. M.,15
16 506 NAYLOR, G. J. 2012. Body plan convergence in the evolution of skates and rays17
18 507 (Chondrichthyes: Batoidea). *Molecular Phylogenetics and Evolution*, **63**, 28–42.19
20
21 50822
23 509 BARRON, E. J. 1987. Eocene equator-to-pole surface ocean temperatures: a significant24
25 510 climate problem? *Palaeoceanography*, **2**, 729–739.26
27
28 51129
30 512 BERG, L. S. 1940. Classification of fishes both recent and fossil. *Travaux de l'Institut*31
32 513 *Zoologique de l'Académie des Sciences de l'U.R.S.S.*, **5**, 85–517.33
34
35 51436
37 515 BONAPARTE, C. L. J. L. 1838. Selachorum tabula analytica. *Nuovi Annali Scienze*38
39 516 *Naturali*, **2**, 195–214.40
41
42 51743
44 518 CARVALHO, M. R. and MAISEY, J. G. 1996. Phylogenetic relationships of the Late45
46 519 Jurassic shark *Protospinax* WOODWARD 1919 (Chondrichthyes: Elasmobranchii). 9–46.47
48 520 *In* ARRATIA, G., VIOHL, G. (eds.). *Mesozoic fishes 1 - systematics and paleoecology*. Dr49
50 521 Friedrich Pfeil Verlag, München, Germany, 576 pp.51
52
53
54 52255
56
57
58
59
60

- 1
2
3 523 COMPAGNO, L. J. V. 1973. Interrelationships of living elasmobranches. 15–61. *In*
4
5 524 GREENWOOD, P. H., MILES, R. S. and PATTERSON, C. (eds.). *Interrelationships of*
6
7 525 *fishes*. Linnean Society of London, London, 536 pp.
8
9 526
10
11 527 — 1977. Phyletic relationships of living sharks and rays. *Integrative and Comparative*
12
13 528 *Biology*, **17**, 303–322.
14
15 529
16
17 530 — 2001. Sharks of the world: an annotated and illustrated catalogue of shark species known
18
19 531 to date. *Volume 2. Bullhead, Mackerel and Carpet sharks (Heterodontiformes, Lamniformes*
20
21 532 *and Orectolobiformes)*. Food and Agriculture Organization of the United Nations, Rome,
22
23 533 269 pp.
24
25 534
26
27 535 CUNY, G. and BENTON, M. J. 1999. Early radiation of the Neoselachian sharks in Western
28
29 536 Europe. *GEOBIOS*, **32**, 193–204.
30
31 537
32
33 538 DANIEL, J. F. 1915. The anatomy of *Heterodontus francisci*. II. The endoskeleton. *Journal*
34
35 539 *of Morphology*, **26**, 447–493.
36
37 540
38
39 541 EBERT, D. A., KHAN, M., VALINASSAB, T., AKHILESH, K. V. and TESFAMICHAEL,
40
41 542 D. 2017. *Heterodontus omanensis*. *The IUCN Red List of Threatened Species*.
42
43 543 <<http://dx.doi.org/10.2305/IUCN.UK.2017-2.RLTS.T161720A109916524.en>>. Downloaded
44
45 544 on 18 June 2018.
46
47 545
48
49 546 FELSENSTEIN, J. 1985. Confidence limits on phylogenies: an approach using the bootstrap.
50
51 547 *Evolution*, **39**, 783–791.
52
53
54
55
56
57
58
59
60

- 1
2
3 548
4
5 549 GUINOT, G. and CAVIN, L. 2015. Contrasting “fish” diversity dynamics between marine
6
7 550 and freshwater environments. *Current Biology*, **25**, 2314–2318.
8
9 551
10
11 552 — UNDERWOOD, C., CAPPETTA, H. and WARD, D. 2013. Sharks from the Late
12
13 553 Cretaceous of France and the U.K. *Journal of Systematic Palaeontology*, **11**, 589–671.
14
15 554
16
17 555 HALLAM, A. 1981. The End-Triassic bivalve extinction event. *Palaeogeography,*
18
19 556 *Palaeoclimatology, Palaeoecology*, **35**, 1–44.
20
21 557
22
23 558 — 1990. The end-Triassic mass extinction event. 577–583. In SHARPTON, V. L. and
24
25 559 WARD, P. D. (eds.). *Global catastrophes in Earth history: An interdisciplinary conference*
26
27 560 *on impacts, volcanism, and mass mortality. Geological Society of America Special Paper*
28
29 561 **247**, 644 pp.
30
31 562
32
33 563 — 2001. A review of the broad pattern of Jurassic sea-level changes and their possible
34
35 564 causes in the light of current knowledge. *Palaeogeography, Palaeoclimatology,*
36
37 565 *Palaeoecology*, **167**, 23–37.
38
39 566
40
41 567 HAMMER, Ø., HARPER, D. A. T. and RYAN, P. D. 2001. PAST: Palaeontological
42
43 568 Statistics software package for education and data analysis. *Palaeontologia Electronica*, **4**, 1–
44
45 569 9.
46
47
48
49
50
51
52
53
54 570
55
56
57
58
59
60

- 1
2
3 571 HARVEY, P. H. and PAGEL, M. D. 1991. *The comparative method in evolutionary*
4
5 572 *biology*. Oxford Series in Ecology and Evolution. Oxford University Press, New York, 248
6
7
8 573 pp.
9
10 574
11
12 575 HAY, O. P. 1902. Bibliography and catalogue of the fossil Vertebrata of North America.
13
14 576 *Bulletin of the United States Geological Survey*, **179**, 1–868.
15
16
17 577
18
19 578 HINES, B. R., HOLLIS, C. J., ATKINS, C. B., BAKER, J. A., MORGANS, H. E. G. and
20
21 579 STRONG, P. C. 2017. Reduction of oceanic temperature gradients in the early Eocene
22
23 580 Southwest Pacific Ocean. *Palaeogeography, Palaeoclimatology, Palaeoecology*, **475**, 41–
24
25 581 54.
26
27
28 582
29
30
31 583 HOVESTADT, D. C. 2018. Reassessment and revision of the fossil Heterodontidae
32
33 584 (Chondrichthyes: Neoselachii) based on tooth morphology of extant taxa. *Palaeontos*, **30**, 3–
34
35 585 120.
36
37
38 586
39
40 587 HUMAN, B. A., OWEN, E. P., COMPAGNO, L. J., V. and HARLEY, E. H. 2006. Testing
41
42 588 morphologically based phylogenetic theories within the cartilaginous fishes with molecular
43
44 589 data, with special reference to the catshark family (Chondrichthyes; Scyliorhinidae) and the
45
46 590 interrelationships within them. *Molecular Phylogenetics and Evolution*, **39**, 384–391.
47
48
49 591
50
51 592 HUXLEY, T. H. 1880. On the application of the laws of evolution to the arrangement of the
52
53 593 Vertebrata and more particularly of the Mammalia. *Proceedings of the Zoological Society of*
54
55 594 *London*, **43**, 649–662.
56
57
58 595
59
60

- 1
2
3 596 INOUE, J. G., MIYA, M., LAM, K., TAY, B. H., DANKS, J. A., BELL, J., WALKER, T. I.,
4
5 597 VENKATESH, B. 2010. Evolutionary origin and phylogeny of the modern holocephalans
6
7
8 598 (Chondrichthyes: Chimaeriformes): a mitogenomic perspective. *Molecular Biology and*
9
10 599 *Evolution*, **27**, 2576–2586.
11
12 600
13
14 601 JACQUES, H., VAN WAES, H. 2012. Observations Concerning the Evolution and the
15
16 602 Parasystematic of all the living and fossil Heterodontiformes. *Géominpal Belgica*, **3**, 1–17.
17
18
19 603
20
21 604 KLUG, S. 2010. Monophyly, phylogeny and systematic position of the
22
23 605 †Synchodontiformes (Chondrichthyes, Neoselachii). *Zoological Scripta*, **39**, 37–49.
24
25
26 606
27
28 607 KOKEN, E. 1911. Pisces. In ZITTEL, K. A. (ed.). *Grundzüge der Paläontologie*.
29
30
31 608 *Volume 2*. München, Berlin, Oldenbourg, 142 pp.
32
33 609
34
35 610 KRIWET, J. 2008. A new species of extinct bullhead sharks, *Paracestracion viohli*
36
37 611 (Neoselachii, Heterodontiformes), from the Upper Jurassic of South Germany. *Acta*
38
39 612 *Geologica Polonica*, **58**, 235–241.
40
41
42 613
43
44 614 — and KLUG, S. 2004. Late Jurassic selachians (Chondrichthyes, Elasmobranchii)
45
46 615 from southern Germany: Re-evaluation on taxonomy and diversity. *Zitteliana*, **A44**:
47
48 616 67–95.
49
50
51 617
52
53
54 618 — and KLUG, S. 2008. Diversity and biogeography patterns of Late Jurassic
55
56 619 neoselachians (Chondrichthyes: Elasmobranchii). 55–70. In LONGBOTTOM, A. E.
57
58
59
60

- 1
2
3 620 and RICHTER, M. (eds). *Fishes and the Break-up of Pangaea*. Special Publications of
4
5 621 the Geological Society, London, 372 pp.
6
7
8 622
9
10 623 — KIESSLING, W. and KLUG, S. 2009a. Diversification trajectories and evolutionary
11
12 624 life-history traits in early sharks and batoids. *Proceedings of the Royal Society, Series B*,
13
14 625 **276**, 945–951.
15
16 626
17
18 627 — NUNN, E. V. and KLUG, S. 2009b. Neoselachians (Chondrichthyes, Elasmobranchii)
19
20 628 from the Lower and lower Upper Cretaceous of north-eastern Spain. *Zoological Journal of*
21
22 629 *the Linnean Society*, **155**, 316–347.
23
24
25 630
26
27
28 631 KUMAR, S., STECHER, G. and TAMURA, K. 2016. MEGA7: Molecular Evolutionary
29
30 632 Genetics Analysis version 7.0 for bigger datasets. *Molecular Biology and Evolution*, **33**,
31
32 633 1870–1874.
33
34 634
35
36
37 635 MADDISON, W. P. and MADDISON, D. R. 2018. Mesquite: a modular system for
38
39 636 evolutionary analysis. Version 3.51. <<http://www.mesquiteproject.org>>
40
41
42 637
43
44 638 MAIA, A. M. R., WILGA, C. A. D. and LAUDER, G. V. 2012. Biomechanics of locomotion
45
46 639 in sharks, rays, and chimeras. 125–151. In CARRIER, J. C., MUSICK, J. A. and
47
48 640 HEITHAUS, M. R. (eds.). *Biology of Sharks and Their Relatives II: Biodiversity, Adaptive*
49
50 641 *Physiology, and Conservation*. CRC Press Taylor & Francis Group, Boca Raton, Florida, 666
51
52
53 642 pp.
54
55 643
56
57
58
59
60

- 1
2
3 644 MAISEY, J. G. 1982. Fossil Hornshark Finspines (Elasmobranchii; Heterodontidae) with
4
5 645 Notes on a New Species (*Heterodontus tuberculatus*). *Neues Jahrbuch für Geologie und*
6
7 646 *Paläontologie, Abhandlungen*, **164**, 393–413.
8
9
10 647
11
12 648 — 2012. What is an ‘elasmobranch’? The impact of palaeontology in understanding
13
14 649 elasmobranch phylogeny and evolution. *Journal of Fish Biology*, **80**, 918–951.
15
16 650
17
18 651 — NAYLOR, G. J. P. and WARD, D. J. 2004. Mesozoic elasmobranchs, neoselachian
19
20 652 phylogeny and the rise of modern elasmobranch diversity. 17–56. In ARRATIA, G. and
21
22 653 TINTORI, A. (eds.). *Mesozoic Fishes 3 – Systematics, Paleoenvironments and Biodiversity*.
23
24 654 Dr Friedrich Pfeil Verlag, München, 649 pp.
25
26 655
27
28
29
30
31 656 MALLATT, J. and WINCHELL, C. J. 2007. Ribosomal RNA genes and deuterostome
32
33 657 phylogeny revisited: more cyclostomes, elasmobranchs, reptiles, and a brittle star. *Molecular*
34
35 658 *Phylogenetics and Evolution*, **43**, 1005–1022.
36
37
38 659
39
40 660 MOORE, G. T. and ROSS, C. A. 1994. Kimmeridgian-Tithonian (Late Jurassic) dinosaur
41
42 661 and ammonoid paleoecology from a paleoclimate simulation. *Canadian Society of*
43
44 662 *Petroleum Geologists Memoir*, **17**, 345–361.
45
46
47 663
48
49 664 NAYLOR, G. J. P., CAIRA, J. N., JENSEN, K. R. E., ROSANA, K. M., STRAUBE, N.
50
51 665 and LAKNER, C. 2012. Elasmobranch phylogeny: a mitochondrial estimate based on 595
52
53 666 species. 31–56. In CARRIER, J. C., MUSICK, J. A. and HEITHAUS, M. R. (eds.).
54
55 667 *Biology of Sharks and Their Relatives II: Biodiversity, Adaptive Physiology, and*
56
57 668 *Conservation*. CRC Press Taylor & Francis Group, Boca Raton, Florida, 666 pp.
58
59
60

1
2
3 669

4
5 670 POLLOM, R., BENNETT, R., EBERT, D. A., FERNANDO, S., JABADO, R. W.,

6
7 671 KUGURU, B., SAMOILYS, M. 2019. *Heterodontus ramalheira*. *The IUCN Red List of*

8
9 672 *Threatened Species*. < <http://dx.doi.org/10.2305/IUCN.UK.2019->

10
11 673 [2.RLTS.T44614A140353520.en](http://dx.doi.org/10.2305/IUCN.UK.2019-2.RLTS.T44614A140353520.en). Downloaded on 05 August 2019.

12
13
14 674

15
16 675 POWTER, D. 2007. Conservation biology of the Port Jackson shark, *Heterodontus*

17
18 676 *portusjacksoni*, in New South Wales. Unpublished PhD thesis, University of Newcastle,

19
20 677 [Australia](#), 466 pp.

21
22
23 678

24
25 679 REIF, W. -E. 1976. Morphogenesis, pattern formation and function of the dentition of

26
27 680 *Heterodontus* (Selachii). *Zoomorphologie*, **83**, 1–47.

28
29
30 681

31
32 682 SLATER, T. 2016. Sharks with question marks – impacts of a new fossil on

33
34 683 interrelationships of early bullhead sharks. 68–72. In McNAMARA, M. E. (ed.).

35
36 684 *Palaeontology Newsletter*. The Palaeontological Association, Durham, 88 pp.

37
38
39 685

40
41 686 — ASHBROOK, K. and KRIWET, J. 2019. [Evolutionary relationships among bullhead](#)

42
43 687 [sharks \(Chondrichthyes: Heterodontiformes\)](#). *Dryad Digital Repository*.

44
45 688 <https://doi.org/10.5061/dryad.6p4f83q>

46
47
48 689

49
50 690 SLUIJS, A., SCHOUTEN, S., PAGANI, M., WOLTERING, M., BRINKHUIS, H.,

51
52 691 DAMSTÈ, J. S. S., DICKENS, G. R., HUBER, M., REICHART, G. -J., STEIN, R.,

53
54 692 MATTHIESSEN, J., LOURENS, L. J., PEDENTCHOUK, N., BACKMAN, J., MORAN,

55
56
57
58
59
60

- 1
2
3 693 K. and EXPEDITION 302 SCIENTISTS. 2006. Subtropical Arctic Ocean temperatures
4
5 694 during the Palaeocene/Eocene thermal maximum. *Nature*, **441**, 610–613.
6
7
8 695
9
10 696 SORENSON, L., SANTINI, F. and ALFARO, M. E. 2014. The effect of habitat on modern
11
12 697 shark diversification. *Journal of Evolutionary Biology*, **27**, 1536–1548.
13
14
15 698
16
17 699 STRONG, W. R., Jr. 1989. Behavioral ecology of horn sharks, *Heterodontus francisci*, at
18
19 700 Santa Catalina Island, California, with emphasis on patterns of space utilization. Unpublished
20
21 701 MSc thesis, California State University, California, USA.
22
23
24 702
25
26 703 SWAFFORD, D. L. 2002. PAUP*. Phylogenetic Analysis Using Parsimony (*and
27
28 704 other methods). Version 4. Sinauer Associates, Sunderland, Massachusetts.
29
30
31 705
32
33 706 THIES, D. 1983. Jurazeitliche Neoselachier aus Deutschland und S-England (Jurassic
34
35 707 Neoselachians from Germany and S-England). *Courier Forschungsinstitut Senckenberg*, **58**,
36
37 708 1–116.
38
39
40 709
41
42 710 TYTELL, E. D. 2006. Median fin function in bluegill sunfish *Lepomis macrochirus*:
43
44 711 streamwise vortex structure during steady swimming. *Journal of Experimental Biology*, **209**,
45
46 712 1516–34.
47
48
49 713
50
51 714 WAGNER, J. A. 1857. Charakteristik neuer Arten von Knorpelfischen aus den
52
53 715 lithographischen Schieferen der Umgegend von Solnhofen. *Gelehrte Anzeigen der königlich*
54
55 716 *bayerischen Akademie der Wissenschaften*, **44**, 288–293.
56
57
58 717
59
60

1
2
3 718 WINCHELL, C. J., MARTIN, A. P. and MALLAT^T, J. 2004. Phylogeny of elasmobranchs
4
5 719 based on LSU and SSU ribosomal RNA genes. *Molecular Phylogenetics and Evolution*, **31**,
6
7 720 214–224.

8
9 721

10
11
12 722 **FIGURES**

13
14 723 FIG. 1. Geological map of Eichstätt, Germany and surrounding areas. Stars indicate locality
15
16 724 from which †*Paracestracion danieli* was excavated.

17
18
19 725

20
21 726 FIG. 2. Photographs of †*Paracestracion danieli*, a complete fossil subadult heterodontiform.
22
23 727 A, UV image. B, counterpart. C, palatoquadrate and Meckel's cartilage with teeth in situ. **D**,
24
25 728 anterior tooth. **E**, parasymphysial tooth. **F**, lateral teeth. **G**, root vascularization of anterior
26
27 729 teeth. **H**, rostral denticles. **I**, cranial denticles. **J**, ventral denticles. **K**, denticles on leading edge
28
29 730 of pelvic fin. Scale bars represent: 1 cm (**A–C**); 0.5 mm (**D–K**).

30
31
32 731

33
34 732 **FIG. 3. A, anterior dorsal fin spine. B, posterior dorsal fin spine. C, dorsal denticles. D, dorsal**
35
36 733 **thorn. Scale bars represent: 1 mm (A–B); 0.5 mm (C–D).**

37
38
39 734

40
41 735 FIG. 4. Tooth morphology of anterior teeth throughout ontogeny for †extinct and extant
42
43 736 heterodontids. The darker grey region denotes the tooth root for †*P. falcifer*. Adapted from
44
45 737 Reif (1976). All scale bars represent 1 mm.

46
47
48 738

49
50 739 **FIG 5. PCA of allometrically scaled distance measurements taken from extinct and extant**
51
52 740 **heterodontids. Ellipses, 95% confidence interval. Adapted from Slater (2016).**

53
54
55 741

56
57
58
59
60

1
2
3 742 FIG 6. Morphometric cladogram of extinct and extant heterodontids. Labels on nodes indicate
4
5 743 bootstrap estimates for ACCTRAN and DELTRAN optimization (the latter in bold). Crosses
6
7
8 744 indicate extinct species. TL, total length; RI, retention index; CI, consistency index.

9
10 745

11 746 FIG 7. A molecular, maximum likelihood phylogeny of extant Heterodontiformes. Bootstrap
12
13
14 747 values and divergence times are indicated (the latter in bold).

15
16
17 748

18 749 TABLE 1. Standing diversity of extinct and extant heterodontiforms through time. Raw data
19
20
21 750 and stratigraphic information taken from Reif (1976) and Hovestadt (2018) are presented with
22
23
24 751 respect to the authors' proposed dental morphotypes. CI, confidence interval; N, number of
25
26 752 species.

27
28
29
30
31 754
32
33
34
35
36
37
38
39
40
41
42
43
44
45
46
47
48
49
50
51
52
53
54
55
56
57
58
59
60

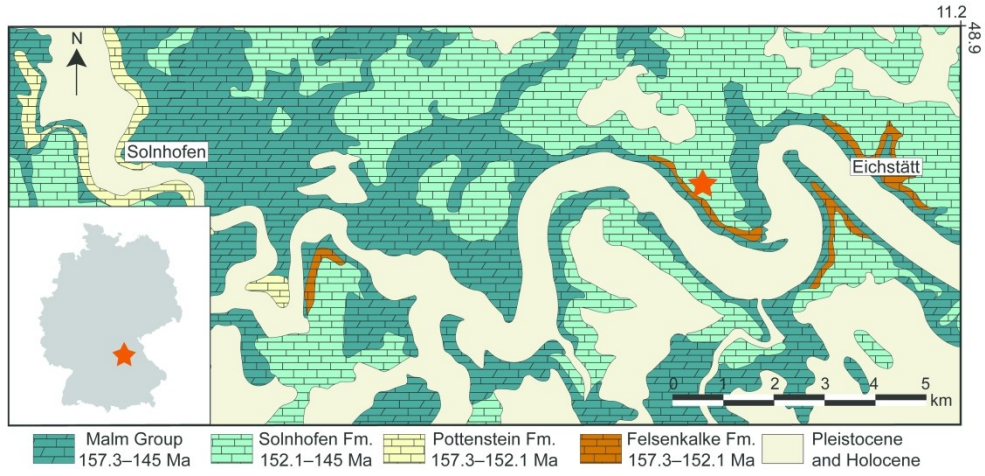


FIG. 1. Geological map of Eichstätt, Germany and surrounding areas. Stars indicate locality from which †Paracestracion danieli was excavated.

160x75mm (600 x 600 DPI)

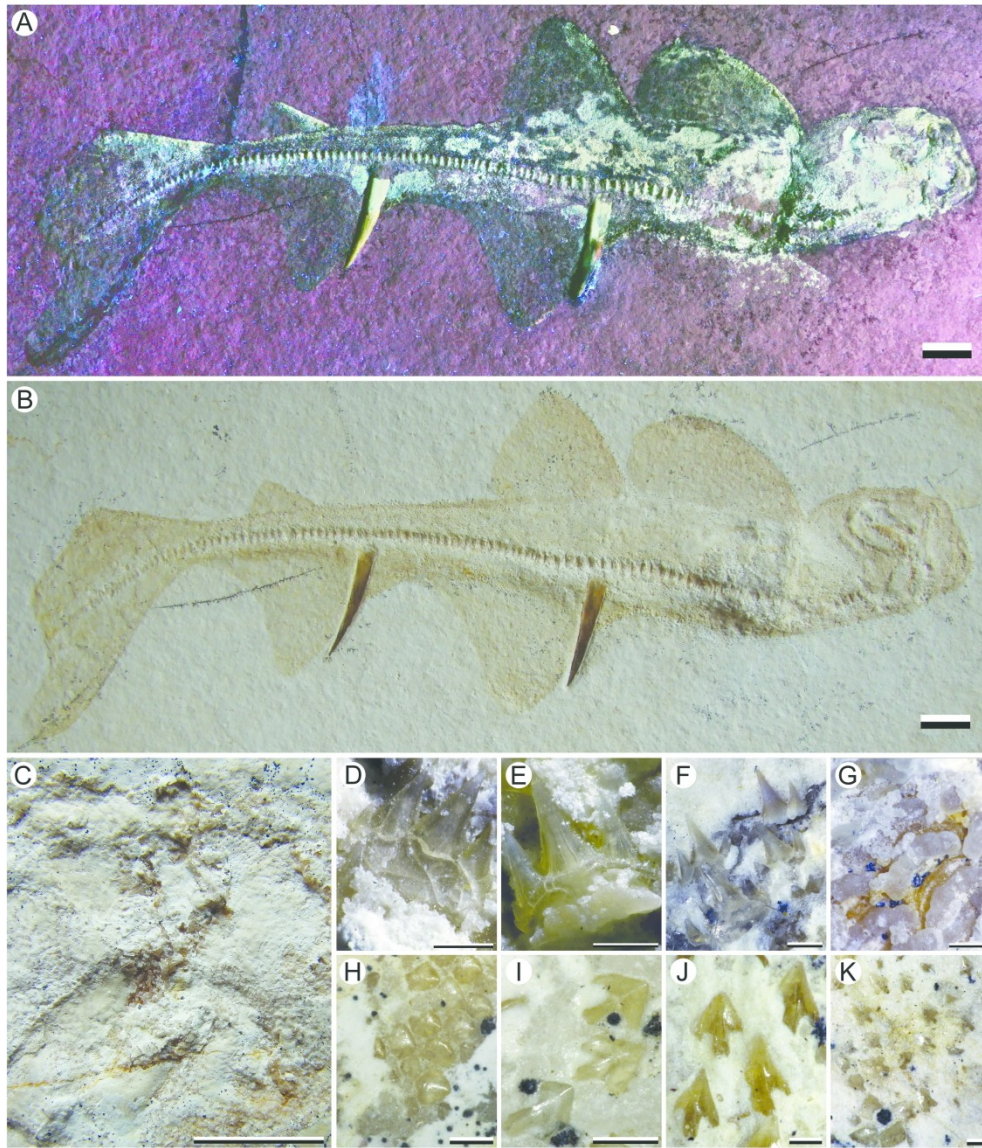


FIG. 2. Photographs of †*Paracestracion danieli*, a complete fossil subadult heterodontiform. A, UV image. B, counterpart. C, palatoquadrate and Meckel's cartilage with teeth in situ. D, anterior tooth. E, parasymphysial tooth. F, lateral teeth. G, root vascularization of anterior teeth. H, rostral denticles. I, cranial denticles. J, ventral denticles. K, denticles on leading edge of pelvic fin. Scale bars represent: 1 cm (A–C); 0.5 mm (D–K).

160x185mm (600 x 600 DPI)

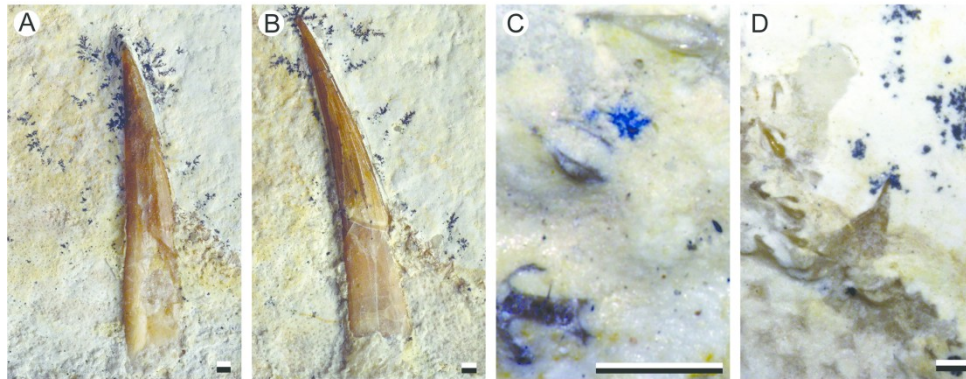


FIG. 3. A, anterior dorsal fin spine. B, posterior dorsal fin spine. C, dorsal denticles. D, dorsal thorn. Scale bars represent: 1 mm (A–B); 0.5 mm (C–D).

160x62mm (600 x 600 DPI)

1
2
3
4
5
6
7
8
9
10
11
12
13
14
15
16
17
18
19
20
21
22
23
24
25
26
27
28
29
30
31
32
33
34
35
36
37
38
39
40
41
42
43
44
45
46
47
48

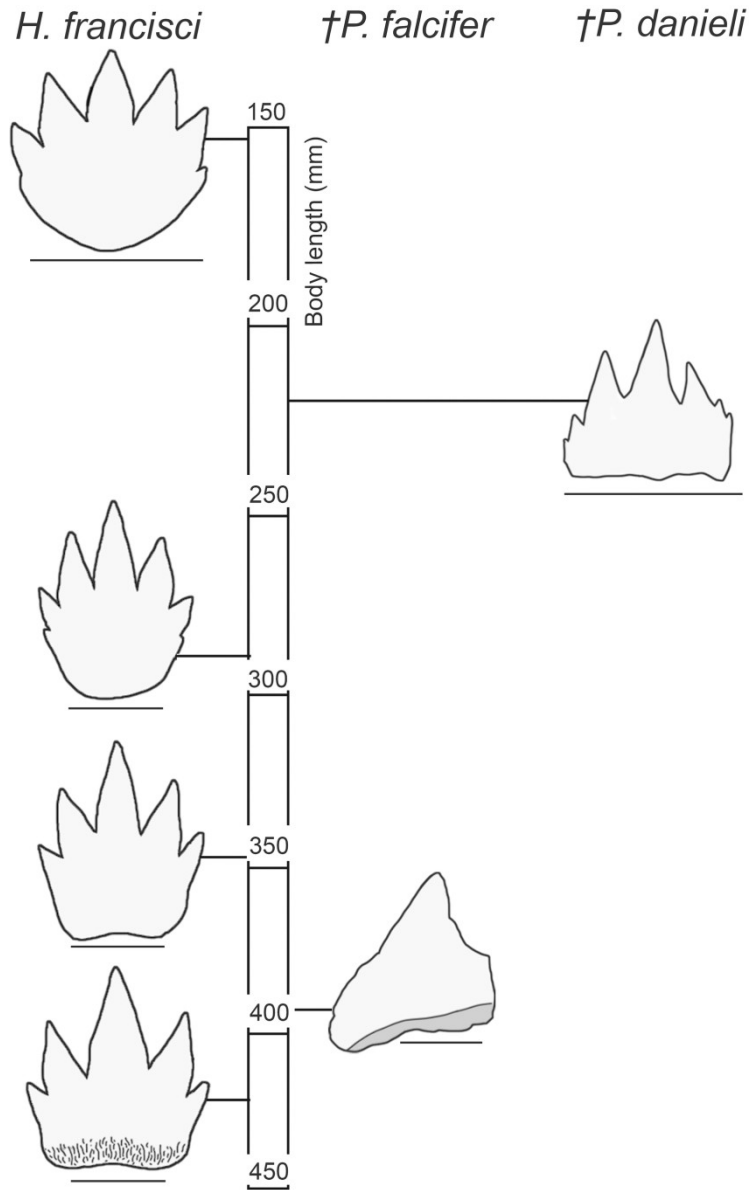


FIG. 4. Tooth morphology of anterior teeth throughout ontogeny for †extinct and extant heterodontids. The darker grey region denotes the tooth root for †*P. falcifer*. Adapted from Reif (1976). All scale bars represent 1 mm.

80x115mm (600 x 600 DPI)

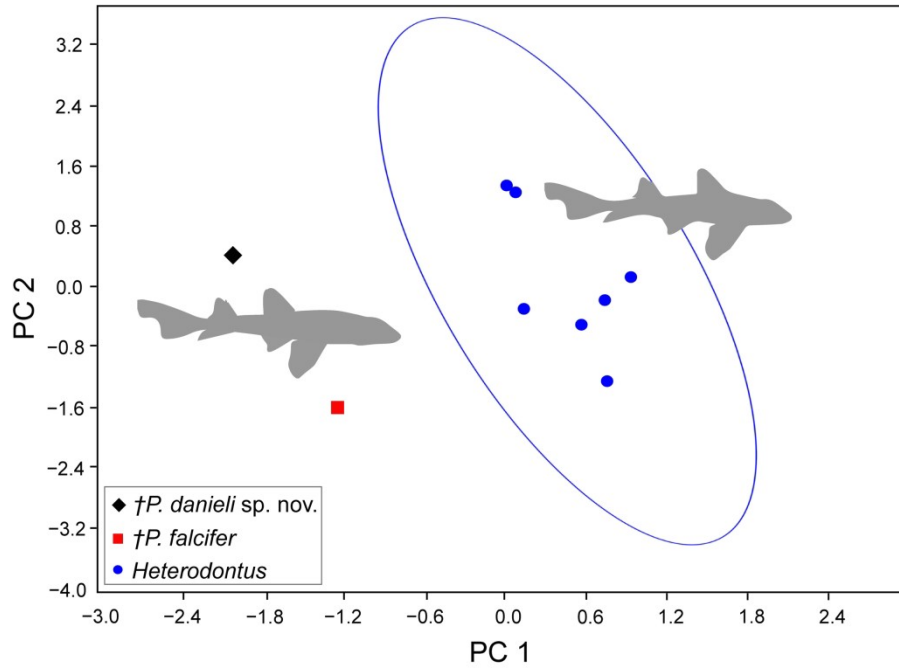


FIG 5. PCA of allometrically scaled distance measurements taken from extinct and extant heterodontids. Ellipses, 95% confidence interval. Adapted from Slater (2016).

109x75mm (600 x 600 DPI)

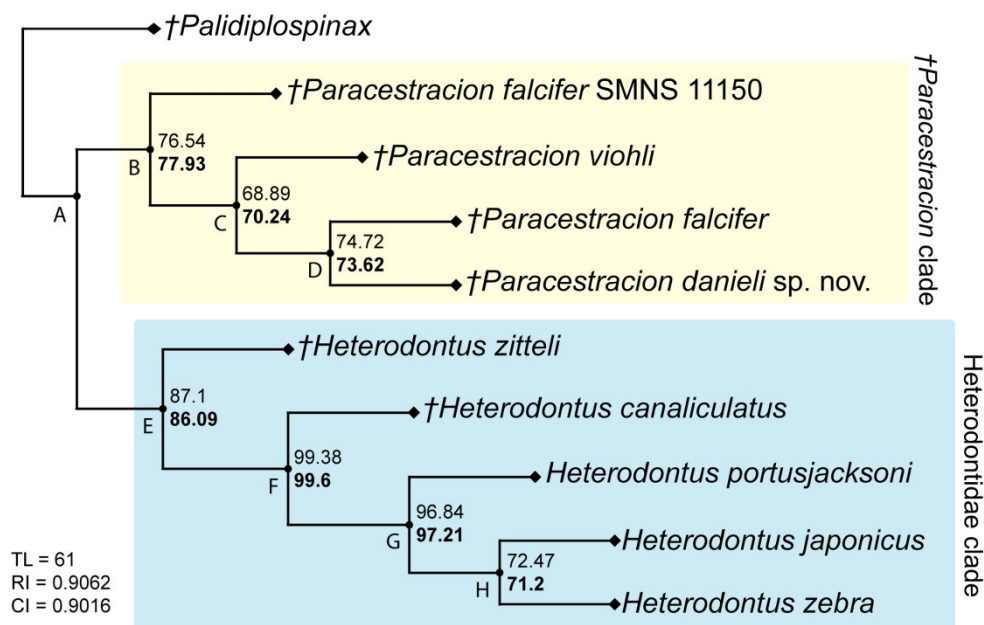


FIG 6. Morphometric cladogram of extinct and extant heterodontids. Labels on nodes indicate bootstrap estimates for ACCTTRAN and DELTRAN optimization (the latter in bold). Crosses indicate extinct species. TL, total length; RI, retention index; CI, consistency index.

110x75mm (600 x 600 DPI)

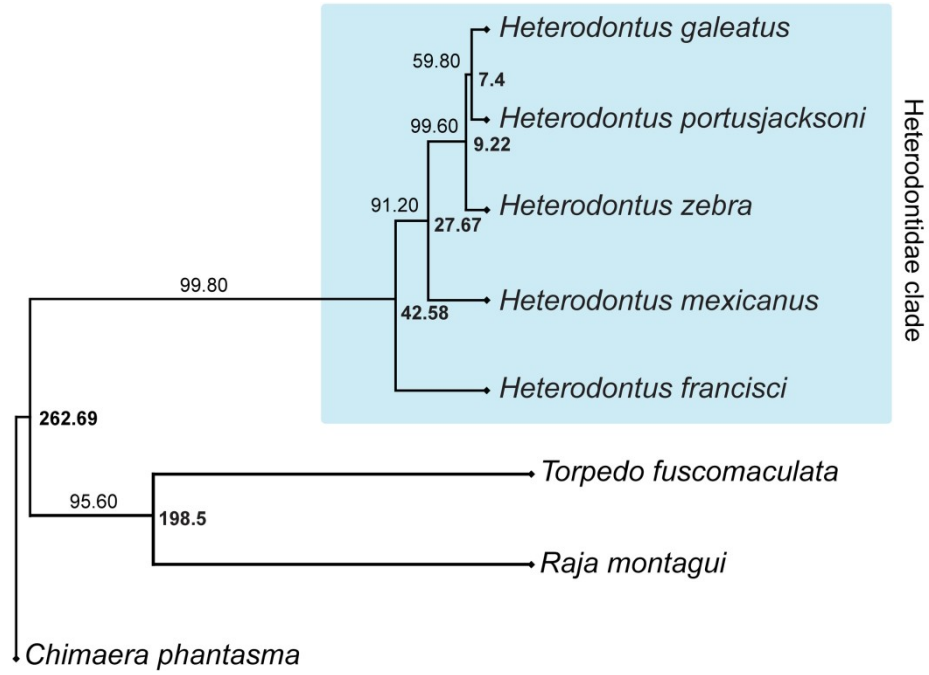


FIG 7. A molecular, maximum likelihood phylogeny of extant Heterodontiformes. Bootstrap values and divergence times are indicated (the latter in bold).

110x75mm (600 x 600 DPI)

	Morphotype			N		Total species (%)	Upper and lower limits of 95% CI (%)
	1	2	?	Epoch	Series		
Recent	3	6		9	9	15.8	-8.98/+10.05
Pliocene	1	1		2	7	12.3	-7.82/+9.19
Miocene	1	4		5			
Oligocene	1			1	10	17.5	-9.33/+10.46
Eocene	4	3		7			
Palaeocene	1	1		2			
Maastrichtian	1	1	2	3	15	26.3	-11.06/+11.84
Campanian	1			1			
Santonian	1			1			
Coniacian							
Turonian		1		1			
Cenomanian	4	4	1	9			
Aptian/Albian		1	1	2	5	8.8	-6.72/+7.97
Barremian			1	1			
Hauterivian							
Valanginian			2	2			
Berriasian							
Late Jurassic				6	6	10.5	-7.37/+8.67
Middle Jurassic				4	4	7	-5.89/+7.39
Early Jurassic				1	1	1.8	-5.89/+7.39
Total species					57		

1
2
3
4
5
6
7
8
9
10
11
12
13
14
15
16
17
18
19
20
21
22
23
24
25
26
27
28
29
30
31
32
33
34
35
36
37
38
39
40
41
42
43
44
45
46
47
48
49
50
51
52
53
54
55
56
57
58
59
60